Original Article

NRF1 Alleviated Oxidative Stress of Glioblastoma Cells by Regulating NOR1

(GBM / NOR1 / NRF1 / oxidative stress)

JIALI WANG[1], SHUAI CHEN[2], WANG XIANG[3], QING ZHU[4], NIANJUN REN[2]

[1]Department of Colon and Rectal Surgery, Hunan Cancer Hospital and The Affiliated Cancer Hospital of Xiangya School of Medicine, Central South University, Changsha 410013, Hunan, China
[2]Department of Neurosurgery, Hunan Cancer Hospital and The Affiliated Cancer Hospital of Xiangya School of Medicine, Central South University, Changsha 410013, Hunan, China
[3]Radiologic Diagnosis Center, Hunan Cancer Hospital and The Affiliated Cancer Hospital of Xiangya School of Medicine, Central South University, Changsha 410013, Hunan, China
[4]Department of Pharmacy, Hunan Cancer Hospital and The Affiliated Cancer Hospital of Xiangya School of Medicine, Central South University, Changsha 410013, Hunan, China

Abstract. Oxidored-nitro domain-containing protein 1 (NOR1) is a critical tumour suppressor gene, though its regulatory mechanism in oxidative stress of glioblastoma (GBM) remains unclear. Hence, further study is needed to unravel the function of NOR1 in the progression of oxidative stress in GBM. In this study, we evaluated the expression of NOR1 and nuclear respiratory factor 1 (NRF1) in GBM tissue and normal brain tissue (NBT) using quantitative real-time polymerase chain reaction (qRT-PCR) and Western blot (WB), and investigated their relationship. We then induced oxidative stress in U251 cells through H_2O_2 treatment and conducted Cell Counting Kit-8, Transwell and wound healing assays to analyse cell proliferation, invasion and migration. Cell apoptosis was assessed by flow cytometry and TUNEL staining. We also measured the activities of superoxide dismutase and catalase, as well as the level of reactive oxygen species (ROS) using biochemical techniques. Via qRT-PCR and WB, the mRNA and protein expression levels of NOR1 and NRF1 were determined. Chromatin immunoprecipitation (ChIP) assays were applied to validate NRF1's interaction with NOR1. Our results showed that the expression of NOR1 and NRF1 was low in GBM, and their expression levels were positively correlated. H_2O_2-induced oxidative stress reduced NRF1 and NOR1 expression levels and increased the ROS level. The ChIP assay confirmed the binding of NRF1 to NOR1. Overexpression of NRF1 attenuated the inhibitory effect of oxidative stress on the proliferation, migration and invasion of U251 cells, which was reversed by knockdown of NOR1.

Received December 15, 2022. Accepted May 26, 2023.

This study was supported by the General Project of Hunan Provincial Natural Science Foundation of China (2019JJ40182).

Corresponding authors: Nianjun Ren, Department of Neurosurgery, Hunan Cancer Hospital and The Affiliated Cancer Hospital of Xiangya School of Medicine, Central South University, No. 283, Tongzipo Road, Yuelu District, Changsha 410013, Hunan, China. E-mail: rennianjun@hnca.org.cn. Qing Zhu, Department of Pharmacy, Hunan Cancer Hospital and The Affiliated Cancer Hospital of Xiangya School of Medicine, Central South University, No. 283, Tongzipo Road, Yuelu District, Changsha 410013, Hunan, China. Phone: +86 0731 88651812; e-mail: zhuqing@hnca.org.cn

Abbreviations: CAT – catalase, CCK-8 – Cell Counting Kit-8, ChIP – chromatin immunoprecipitation, GBM – glioblastoma, NBT – normal brain tissue, NOR1 – oxidored-nitro domain-containing protein 1, NRF1 – nuclear respiratory factor 1, PBS – phosphate-buffered saline, qRT-PCR – quantitative real-time polymerase chain reaction, ROS – reactive oxygen species, SOD – superoxide dismutase, WB – Western blot.

Introduction

Glioblastoma (GBM) is an aggressive malignant brain tumour of the central nervous system, classified as grade IV astrocytoma (McNamara et al., 2022). The current treatment options for GBM include surgery, radiotherapy, drug therapy (typically chemotherapy combined with temozolomide), and immunotherapies (Asija et al., 2022; Rong et al., 2022; Yuan et al., 2022). Despite significant efforts to develop optimal treatment strategies, GBM patients have a very poor prognosis, with high mortality rates and a median overall survival of only about 15 months (Grochans et al., 2022). Therefore, it is crucial to explore innovative treatment approaches that can improve the prognosis of GBM patients.

Reactive oxygen species (ROS) accumulation, which causes oxidative stress, is a risk factor for the emergence

of GBM (Olivier et al., 2020; Ostrowski and Pucko, 2022). Nuclear respiratory factor 1 (NRF1) is a crucial transcription factor that controls antioxidant defence and is essential for keeping cellular redox homeostasis, preventing oxidative damage and reducing inflammation (Bugno et al., 2015; Zhang and Xiang, 2016). It has been reported that NRF1 is a potential therapeutic target for preventing and treating cancer, neurodegenerative diseases and other disorders (Northrop et al., 2020; Ruvkun and Lehrbach, 2023). Over-expression of NRF1 could up-regulate the expression of ROS scavenging enzymes, allowing tumour cells to maintain low ROS levels, thereby promoting the epithelial mesenchymal transition of breast cancer cells (Sun et al., 2023).

Oxidored-nitro domain-containing protein 1 (NOR1) is a gene expression regulator located in the nucleus with selective tissue-specific expression. It plays a crucial role in various pathological processes such as cancer, inflammatory diseases and Parkinson's disease (Herring et al., 2019). Studies have shown that oxidative stress could induce NOR1 protein expression by activating NRF1 and heat shock factor 1 (HSF1) transcription factors, and NRF1 and HSF1 may participate in the incidence and growth of cancers linked to oxidative stress through the regulation of NOR1 (Li et al., 2011).

This work aims to confirm, through clinical samples and cellular investigations, the relationship between NRF1 and NOR1 with regard to oxidative stress in GBM. The goal is to establish a theoretical foundation for developing antioxidant medications targeting NOR1.

Material and Methods

Tissue samples

Between January 2020 and September 2020, ten specimens of GBM tissue, as well as their adjacent normal brain tissue (NBT), were collected from Hunan Cancer Hospital in accordance with the National Regulation of Clinical Samples in China.

Cell culture and treatment

The human HEB, T98G, U87 and U251 cell lines were obtained from BNCC (Beijing, China) and cultured in Dulbecco's modified Eagle's medium (DMEM) (Sigma, St. Louis, MO) supplemented with 10 % foetal bovine serum (FBS) and 1 % penicillin-streptomycin solution in a humid environment at 37 °C containing 5 % CO_2. Once the cells reached 80–90 % confluence, they were sub-cultured. To induce oxidative stress, U251 cells were treated with various doses of H_2O_2 (0, 50, 100, 150, 200, and 250 μM) for 24 hours, and 100 μM was determined to be the optimal concentration for subsequent experiments. The cells were divided into five groups: Control group (no treatment), Model group (treated with 100 μM H_2O_2 for 24 hours), oe-NC+si-NC group (treated with 100 μM H_2O_2 for 24 hours and transfected with empty plasmid for 48 hours), oe-NRF1 group (treated with 100 μM H_2O_2 for 24 hours and transfected with oe-NRF1 plasmid for 48 hours), and oe-NRF1+si-NOR1 group (treated with 100 μM H_2O_2 for 24 hours and transfected with oe-NRF1 plasmid and si-NOR1 plasmid for 48 hours).

Cell transfection

Cells were transfected with plasmid pcDNA3.1 NRF1 (HG-HO005011, HonorGene, Changsha, China) and siRNA NOR1 (HG-Si173200, HonorGene) using Lipofectamine 2000 (11668019, Invitrogen, Waltham, MA) according to the manufacturer's instructions, with oe-NC and si-NC serving as the controls. The normal culture medium was changed for continued culture after 6 h of transfection, and relevant detection was carried out 48 hours later.

Quantitative real-time polymerase chain reaction (qRT-PCR)

TRIzol reagent (V900483, Sigma) was used to extract total cellular RNA. The concentration (absorbance at 260 nm) and purity (absorbance ratio 260/280) of RNA were measured using a NanoDrop instrument (Thermo Scientific, Waltham, MA). The RNA was used as a template reverse transcribed to cDNA using the mRNA reverse transcription kit (CW2569, CWBIO, Beijing, China). UltraSYBR Mixture (CW2601, CWBIO) was shown in PCR utilizing a fluorescence quantitative PCR instrument (PIKOREAL96, Thermo). The $2^{-\Delta\Delta Ct}$ technique was employed to determine the relative expression of NOR1 and NRF1 with β-actin as an internal control. All primers were designed with Primer-BLAST online and obtained by Tsingke Biotechnology. Primer sequences of target genes are shown in Table 1.

Cell Counting Kit-8 (CCK-8)

The CCK-8 method was used to assess cell proliferation (NU679, Dojindo, Kumamoto, Japan). Approximately 5×10^4 cells were seeded per well in a 96-well plate (0030730119, Eppendorf, Hamburg, Germany), with each group having three replicates. After 24 hours of cell growth, 30 μl of CCK-8 solution was added to each well and incubated for 4 hours at 37 °C. The absorbance at 450 nm was then tested using a Bio-Tek microplate (MB-530, Heales, Shenzhen, China).

Table 1. Primer sequences

Gene	Primer sequences	Length
β-actin	F ACCCTGAAGTACCCCATCGAG	224 bp
	R AGCACAGCCTGGATAGCAAC	
NOR1	F CTTTGCAACGCTGACGGTG	244 bp
	R AGAGCTGTCCCGAAATCTGC	
NRF1	F TCCTGGTCCAGAACTTTACACA	124 bp
	R ATTTGGGTCACTCCGTGTTCC	

Transwell assay

The trypsin-digesting solution was used to digest the cells (AWC0232, Abiowell, Changsha, China). The cell density was set to approximately 2×10^6/ml, and the cells were placed in serum-free DMEM. A volume of 200 µl serum-free medium was added to the upper chamber of an 8 µm pore size Transwell plate (3428, Corning, Cambridge, MA), followed by 100 µl of cell suspension. The lower chamber was filled with a complete medium containing 10 % FBS. The cells on the upper side of the membrane were cultivated for 48 hours before being washed with phosphate-buffered saline (PBS). The cells that migrated to the lower chamber were dyed with 0.1 % crystal violet (AWC0333, Abiowell) and treated with 4 % paraformaldehyde (N1012, NCM Biotech, Suzhou, China). An inverted microscope (DSZ2000X, Cnmicro, Beijing, China) was used to observe the cells. The staining was washed with acetic acid, and the absorbance was measured at 550 nm using a Bio-Tek microplate reader.

Wound healing assay

Once the cells reached the confluence of over 90 %, they were seeded into a 6-well culture plate. To eliminate any detached cells, the plate was gently scraped with a sterile plastic pipette tip and then rinsed with PBS. A single wound in the middle of the cell monolayer was created using a sterile pipette tip. The wound was then monitored and imaged at 0, 24, and 48 hours post-wounding. The degree of wound closure was calculated by measuring the percentage reduction in initial scratch area at each time point.

TUNEL staining

TUNEL analyses were performed with chamber slides containing U251 cells. After an overnight culture, the cells were washed with PBS three times and fixed in 4 % paraformaldehyde for 30 min. TUNEL assays were carried out using the TUNEL kit (40306ES50, Yeasen, Shanghai, China) as per the manufacturer's instructions. Fluorescence microscopy (BA410T, Motic, Xiamen, China) was then used to observe cell apoptosis. To determine the quantity of TUNEL-positive cells, three fields were randomly selected.

Flow cytometry

The cells were harvested by centrifugation at $1{,}216 \times g$ for 5 min and then washed with PBS. Following that, the Annexin V-APC apoptosis detection kit (KGA1019, KeyGen BioTECH, Nanjing, China) was applied. Suspension cells were mixed with 500 µl of binding buffer and then combined with 5 µl of Annexin V-APC and 5 µl of propidium iodide. This mixture was left to incubate at 4 °C for 10 min in the dark. To identify cell apoptosis, flow cytometry (A00-1-11102, Beckman Coulter, Brea, CA) was applied.

Chromatin immunoprecipitation (ChIP) assay

Following instructions of the manufacturer, the ChIP experiment was completed using the CHIP kit (ab500, Abcam, Cambridge, UK). The cells were first cross-linked with 1.1 % formaldehyde for 10 min at room temperature and then quenched with glycine. The cells were then lysed using a buffer containing protease inhibitors, and the chromatin was broken using ultrasonic treatment. The sheared chromatin was incubated with either anti-NRF1 (ab175932, Abcam) or anti-Histone H3 (ab1791, Abcam) antibody after pre-clearing with Protein A agarose beads for 1 h. The mixture was rotated overnight at 4 °C. DNA purification was performed as recommended by the manufacturer. The JASPAR transcription factor binding profile database was utilized to find the anticipated NRF1 binding locations. Real-time PCR with SYBR green was conducted to confirm the NRF1 promoter-specific regions using the primer sets shown in Table 2. The Assay Site IP Fold Enrichment above the sample-specific background (linear conver-

Table 2. Primer sequences

Gene	Primer sequences	Length
NOR1-ChIP1	F CGCCCGAGACCCGGCTAAA	143 bp
	R CGCCCCTTCTCCATTCAACGC	
NOR1-ChIP2	F GGGAACCTACTCCGCTATCT	201 bp
	R AAGTTGACCCAGCCGAGA	
NOR1-ChIP3	F GGGAGGAGGAATGATTTGC	225 bp
	R TTACTGGGTGCGTGTTTCA	
NOR1-ChIP4	F TGTGAAACACGCACCCAGTA	187 bp
	R CAGCTTCTGACCAGCTCCAGT	
NOR1-ChIP5	F CTGGCGGAGCCTTCCCTTT	120 bp
	R CGGGTGGAGTAGAGTTGGAGGAG	
NOR1-ChIP6	F CGGCGGAGTTTCCATTGTG	180 bp
	R ATAGAGTGCCTGGAATGCGAGA	

sion of the first ΔΔCt) was calculated by the kit using the following equation: Fold Enrichment = $2^{(-\Delta\Delta Ct\ [ChIP/NIS])}$ (Sun et al., 2018; Pla-Martín et al., 2020).

Western blot (WB)

The experimental procedures were conducted as previously described (Xu et al., 2012). A protease inhibitor (583794, Gentihold, Beijing, China) was added to buffer RIPA (AWB0136, Abiowell) before U251 cells were lysed. The bicinchoninic acid (BCA) method was used to measure protein concentrations. Equal amounts of protein (20 μg/lane) were separated by sodium dodecyl sulphate-polyacrylamide gel electrophoresis (SDS-PAGE) and then transferred to polyvinylidene difluoride (PVDF) membranes. Membranes were incubated with primary antibodies overnight at 4 °C after being blocked with 5 % (w/v) non-fat dry milk for 90 min. The primary antibodies used were NOR1 (ab259939, 1 : 1000, Abcam), NRF1 (66832-1-Ig, 1 : 5000, Proteintech, Rosemont, IL) and β-actin (66009-1-Ig, 1 : 5000, Proteintech). After washing the membranes with PBS with Tween (PBST) three times, they were incubated with secondary antibodies provided by Proteintech, including HRP goat anti-mouse IgG (SA00001-1, 1 : 5000) and HRP goat anti-rabbit IgG (SA00001-1, 1 : 6000), for 1 h. Then, the antibody complexes were detected by the electrochemiluminescence (ECL) method. After washing the PVDF membrane five times with PBST, enhanced chemiluminescence ECL reagent (AWB0005, Abiowell) was added and the membrane was subjected to X-ray film for signal detection.

Biochemical assays

For biochemical determination, the first step was to re-suspend the cells in pre-cooled PBS. After undergoing ultrasound treatment, the supernatant was used as the sample for detection. The Nanjing Jiancheng Institute of Biological Engineering supplied the ROS test kit (E004-1-1), superoxide dismutase (SOD) assay kit (A001-3-2), and catalase (CAT) assay kit (A007-1-1).

Statistical analysis

We conducted at least three replicates for all aforementioned tests. Using the statistical software GraphPad Prism 8.0, we analysed the outcomes and expressed measurement data as mean ± standard deviation. Our analysis involved the use of Student's *t*-test and one-way analysis of variance (ANOVA) to compare two or more groups. Moreover, the correlation analysis was employed to evaluate the relationship between NRF1 and NOR1. Our results indicated a significant difference at $P < 0.05$.

Results

Low expression of NOR1 and NRF1 in GBM

qRT-PCR analysis was conducted to assess the expression of NRF1 and NOR1 in both NBT and GBM tissues. The results showed a considerable decrease in the levels of NOR1 and NRF1 expression in GBM tissues as compared to those in NBT tissues (Fig. 1A). The study also investigated the correlation between NOR1 and NRF1 expression levels and discovered a positive correlation between them (Fig. 1B). In addition, WB results showed low expression of NOR1 and NRF1 in GBM tissues, which was consistent with the results of qRT-PCR (Fig. 1C). Furthermore, the study evaluated the expression level of NOR1 in HEB, T98G, U87 and U251 cell lines using qRT-PCR. The results indicated that the expression level of NOR1 in T98G, U87 and U251 cell lines was significantly lower compared to that observed in the HEB cell line, with the lowest expression level being in the U251 cell line (Fig. 1D). As a result, the U251 cell line was chosen for subsequent experiments.

Construction of H_2O_2-induced oxidative stress model in vitro

Then, U251 cells were treated with H_2O_2 to construct an H_2O_2-induced oxidative stress model *in vitro*. CCK-8 analysis revealed that there was no significant change in cell proliferation at H_2O_2 concentrations of 50–100 μM compared to the Control group, but there was a significant decrease in proliferation at concentrations of 150–250 μM (Fig. 2A). Therefore, a concentration of 100 μM was chosen for subsequent experiments. TUNEL staining showed that the rate of cell apoptosis did not differ significantly between the Control group and the Model group (Fig. 2B). The level of ROS and the activities of SOD and CAT were detected using specific kits, revealing a significant reduction in the activities of SOD and CAT in the Model group along with an increase in the ROS level (Fig. 2C–E). Furthermore, qRT-PCR data indicated that NOR1 and NRF1 expression levels in cells were significantly reduced after H_2O_2 treatment (Fig. 2F).

NRF1 was a novel NOR1-binding partner

The *NOR1* promoter possessed six potential NRF1-binding sites, which we discovered using transcription factor binding database Jaspar (Table 2). To confirm whether NRF1 directly interacts with these predicted binding sites, we performed ChIP analysis. After ultrasonication, we observed that the molecular weights of DNA fragments were concentrated within the 100–250 bp range (Fig. 3A). We then used a rabbit polyclonal anti-NRF1 antibody (IP) or normal rabbit IgG (IgG) to investigate NRF1 binding at specific locations within the *NOR1* promoter region. We focused on six locations, ranging from -143 kb to -225 kb from the promoter region. Among these, only *NOR1*-ChIP2, *NOR1*-ChIP3 and *NOR1*-ChIP6 exhibited NRF1 binding with a Fold Enrichment greater than 1, as indicated by the ChIP analysis (Fig. 3B). The findings suggest that only these three sites directly interact with NRF1.

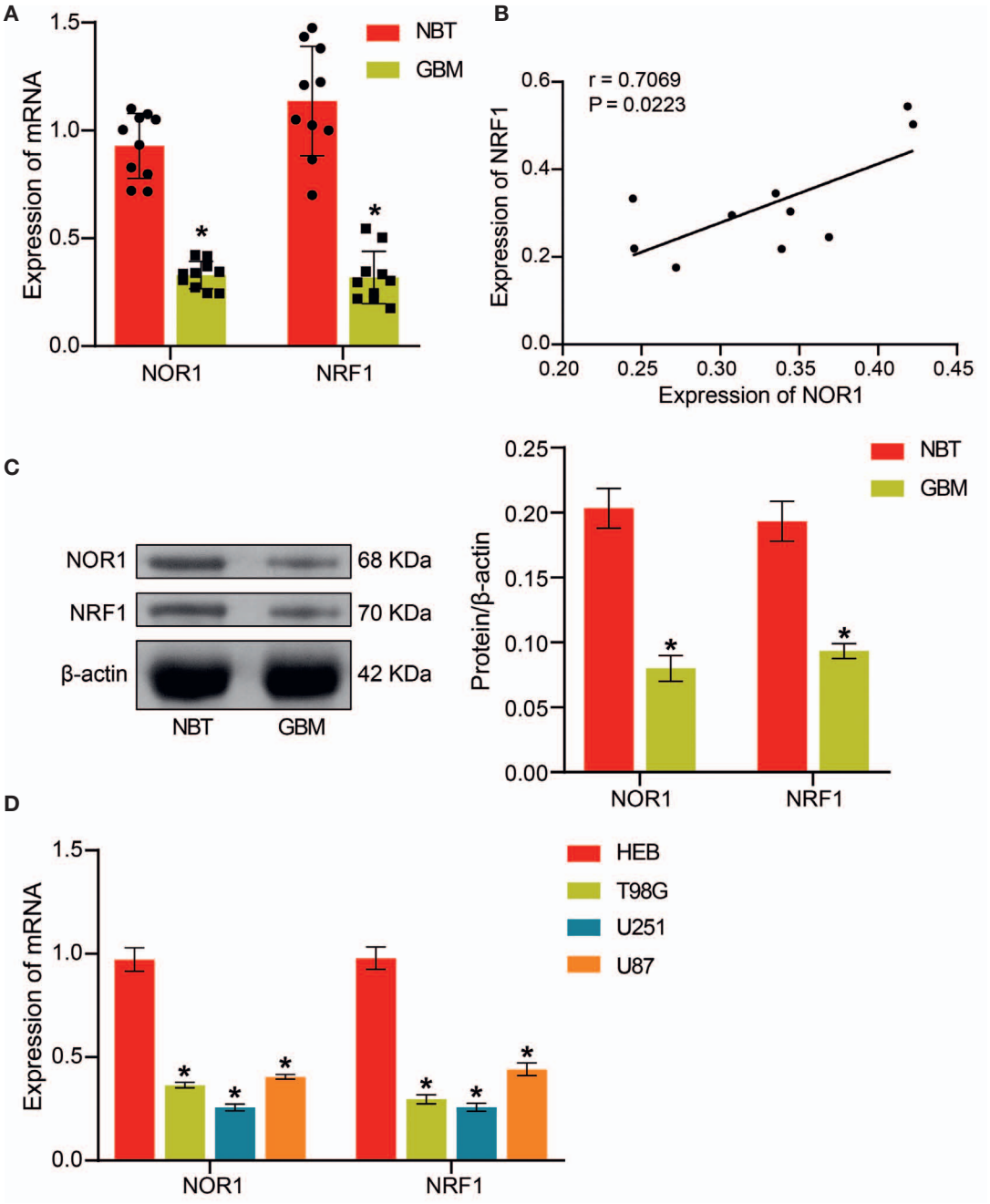

Fig. 1. Low expression of NOR1 and NRF1 in GBM
(A) Assessment of NOR1 and NRF1 expression in NBT and GBM tissues by qRT-PCR. **(B)** Correlation between the expression levels of NRF1 and NOR1. **(C)** Detection of the protein expression of NOR1 and NRF1 by WB. *P < 0.05 vs the NBT tissue. **(D)** Assessment of NOR1 expression in HEB, T98G, U87 and U251 cell lines by qRT-PCR. *P < 0.05 vs the HEB cell line.

Knockdown of NOR1 could alleviate the anti-oxidative stress effect of NRF1 on U251 cells

To further investigate the effects and regulatory mechanisms of NRF1 and NOR1 on H_2O_2-induced U251 cells, we performed experiments with over-expression of NRF1 and knockdown of *NOR1*. Results from qRT-PCR and WB tests showed that the expression levels of NRF1 and NOR1 in the oe-NRF1 group were significantly elevated compared to those in the oe-NC+si-NC group. Notably, the expression level of NRF1 in the oe-NRF1+si-NOR1 group increased, while the expression level of NOR1 did not exhibit significant changes (Fig. 4A and B). In the CCK-8 experiment, we observed that the cell proliferation ability in the Model group decreased significantly compared to the Control group, while the oe-NRF1 group showed a significant increase in cell proliferation ability compared to the oe-NC+si-NC group.

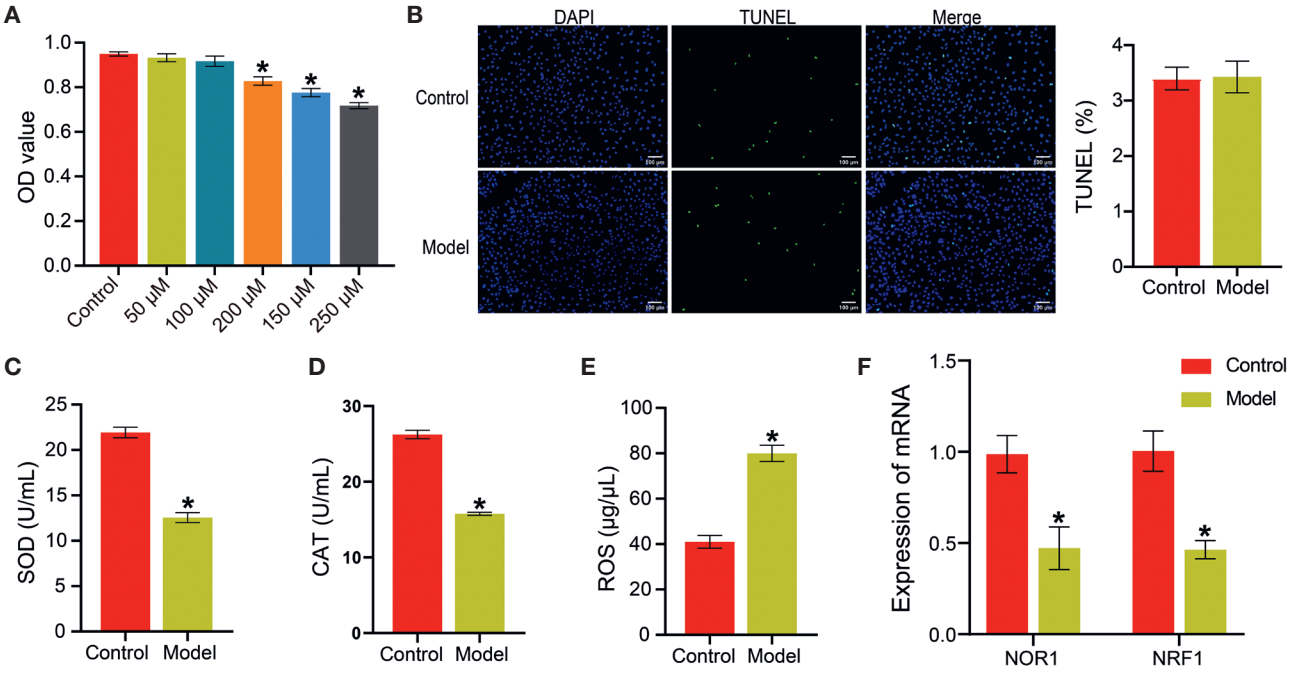

Fig. 2. Construction of H_2O_2-induced oxidative stress model *in vitro*
(A) CCK-8 assay was applied to detect cell proliferation. **(B)** Representative images and value of apoptosis in the Control and Model groups were assessed by TUNEL assay. Scale bar = 100 μm. **(C–E)** To test the levels of SOD, CAT and ROS, the biochemical assay kit was applied. **(F)** The expression levels of NOR1 and NRF1 in U251 cells were detected by qRT-PCR. *P < 0.05 vs the Control group.

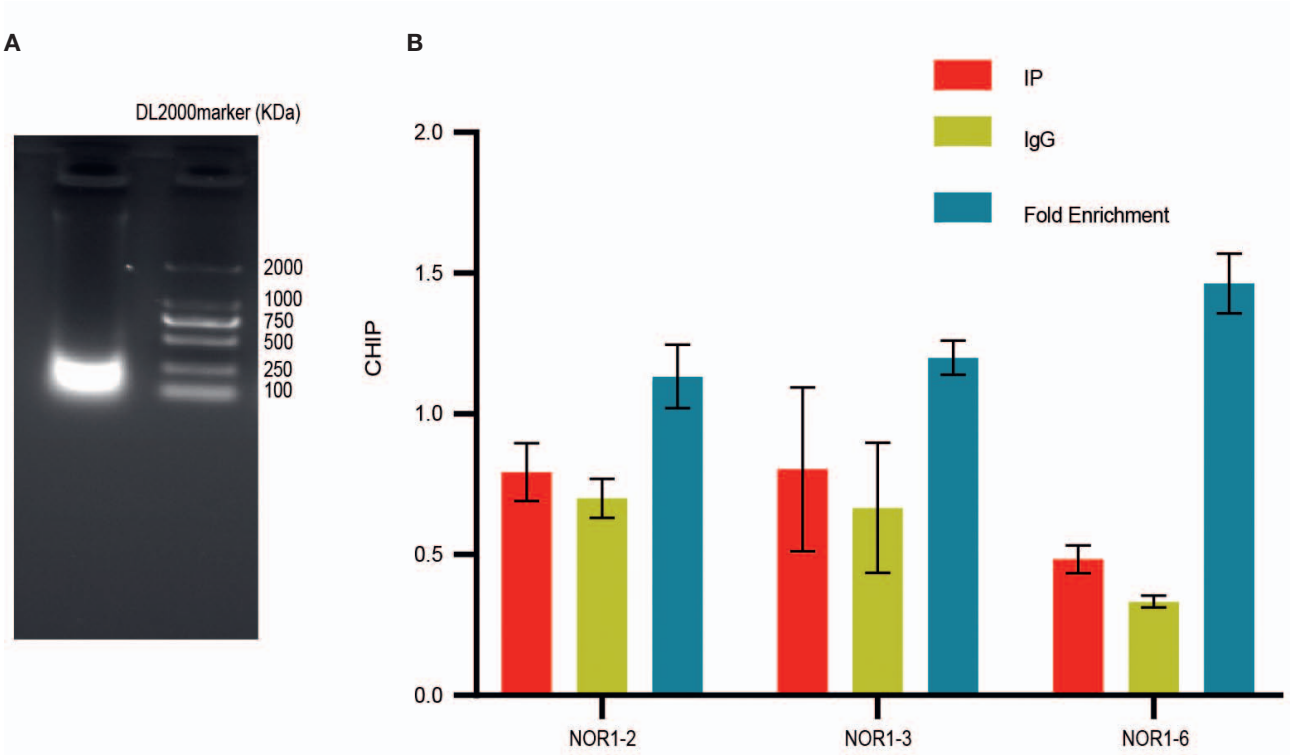

Fig. 3. NRF1 was a novel NOR1-binding partner.
(A) Size distribution of DNA fragments after cell cross-linking by ultrasound. **(B)** Transcriptional factor NRF1 was confirmed to bind promoters *NOR1-2*, *NOR1-3*, and *NOR1-6*.

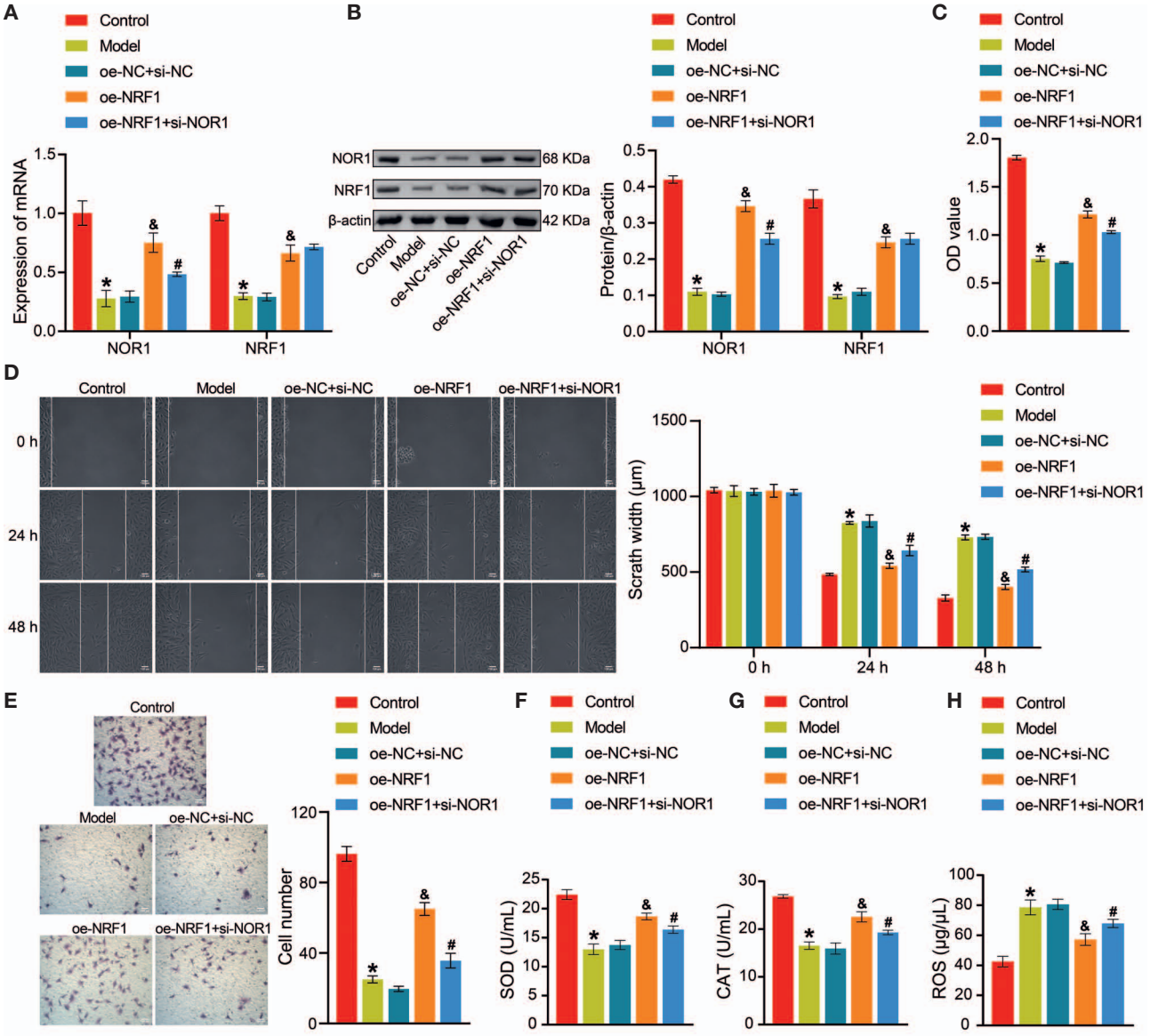

Fig. 4. Knockdown of *NOR1* could alleviate the anti-oxidative stress effect of NRF1 on U251 cells.
(A) The mRNA expression of NRF1 and NOR1 was evaluated by qRT-PCR. **(B)** WB was applied to measure the protein expression of NRF1 and NOR1. **(C)** CCK-8 assay of cell proliferation. **(D)** Scratch width value and representative images of migration were assessed by Transwell assay. Scale bar = 100 μm. **(E)** Representative images and cell numbers were detected by wound healing assay. Scale bar = 100 μm. **(F–H)** To test the levels of SOD, CAT and ROS, biochemical assays were applied. *P < 0.05 vs Control, &P < 0.05 vs oe-NC+si-NC, #P < 0.05 vs oe-NRF1.

However, further knockdown of *NOR1* impaired the promoting effect of oe-NRF1 on the cell proliferation (Fig. 4C). The wound healing experiment results showed that the scratch width of the Model group was significantly increased compared to the Control group, while the oe-NRF1 group had a significantly smaller scratch width than the oe-NC+si-NC group. However, the outcome caused by oe-NRF1 was reversed by further knockdown of *NOR1* (Fig. 4D). In the Transwell cell invasion experiment, the number of cells passing through the Transwell chamber in the Model group was significantly lower than that in the Control group, and the number of cells in the oe-NRF1 group was higher than that in the oe-NC+si-NC group. Interestingly, the further knockdown of *NOR1* reversed the effect of oe-NRF1 (Fig. 4E). Furthermore, ELISA results indicated that compared to the oe-NC+si-NC group, the levels of SOD and CAT in the oe-NRF1 group were increased, while the levels of ROS were reduced significantly. However, in the oe-NRF1+si-NOR1 group, we observed the opposite trend from the oe-NRF1 group (Fig. 4F–H). Overall, these results suggest that over-expression of NRF1 could alleviate the inhibitory effect of H_2O_2-induced oxidative stress on the proliferation, migration, and invasion of U251 cells, which might be reversed by knockdown of *NOR1*.

Discussion

GBM is a highly prevalent and deadly malignant neuroepithelial tumour of the adult central nervous system (Grochans et al., 2022; McNamara et al., 2022). Oxidative stress, which leads to changes in gene expression, cell proliferation and apoptosis, plays a critical role in the occurrence and development of tumours (Jelic et al., 2021). In the current research, we found that the expression of NOR1 and NRF1 was low in GBM, and their expression levels were positively correlated. Overexpression of NRF1 could alleviate the inhibitory effect of H_2O_2-induced oxidative stress on the proliferation, migration, and invasion of U251 cells, which might be reversed by knockdown of *NOR1*.

Oxidative stress damage is a major cause of cellular damage that results from the accumulation of ROS. ROS can cause oxidation of DNA, proteins and lipids, as well as damage to cellular organelles, which ultimately leads to tumorigenesis when the damaged cells accumulate to a certain level (Hayes et al., 2020; Kuo et al., 2022). In our study, we found that H_2O_2-induced oxidative stress inhibited proliferation, migration and invasion of U251 cells and promoted cell apoptosis, which was consistent with the results of Dalavaikodihalli et al. (2019). NRF1, a redox-sensitive transcription factor, is vital for maintaining healthy redox homeostasis (Yuan et al., 2018; Zhang et al., 2020). Deletion of NRF1 function leads to a sharp increase in ROS and oxidative damage (Hu et al., 2022). Our study found that NRF1 was down-regulated in GBM at the mRNA level, which was further supported by the up-regulation of NRF1 and NOR1 protein expression in GBM tissue. In addition, we found that over-expression of NRF1 alleviated the inhibitory effects of H_2O_2-induced oxidative stress on cell proliferation, migration and invasion while increasing the activities of SOD and CAT.

NOR1 is a newly identified regulator involved in the oxidative stress response, linked to the emergence of oxidative stress-related tumours. It has been shown that there are binding sites for NRF1 and HSF1 on *NOR1*, and oxidative stress could induce *NOR1* expression by activating the transcription of *NRF1* and *HSF1*. A study by Li et al. (2011) investigated the impact of NOR1 on HNE1 cell viability in the presence of oxidative stress, finding that over-expression of NOR1 inhibited cell viability and promoted apoptosis. However, the role of NOR1 in oxidative stress in GBM has yet to be studied. In this study, we confirmed the binding of NRF1 to *NOR1* by ChIP assay and constructed a *NOR1* knockdown vector. Our results showed that interfering with NOR1 expression reduced the anti-oxidative stress effect of NRF1 on U251 cells. These findings provide insight into the regulatory mechanisms of NOR1 in the context of oxidative stress in GBM.

To summarize, the findings suggest that NRF1 could alleviate the effects of H_2O_2-induced oxidative stress in U251 cells by regulating NOR1 expression. This study highlights the potential of NOR1 as a promising therapeutic target for GBM treatment.

Conflict of interests

The authors declare that they have no competing interests.

Data availability statement

The data used to support the findings of this study are available from the corresponding author upon request.

Ethics approval and consent to participate

The study was approved by the Hunan Cancer Hospital Ethics Committee. The research was conducted according to the World Medical Association Declaration of Helsinki. All the information about the study will be fully explained to the subjects by the researchers. All the participants provided informed consent before sampling.

Author contributions

Jiali Wang and Qing Zhu made significant contributions to conceptualization, data curation, investigation, methodology, validation and writing of the original draft. Shuai Chen and Wang Xiang contributed to conceptualization, formal analysis, investigation, software, validation and writing of the original draft. Nianjun Ren contributed significantly to conceptualization, funding acquisition, project administration, supervision and review. All authors contributed to the article and approved the submitted version.

References

Asija, S., Chatterjee, A., Yadav, S., Chekuri, G., Karulkar, A., Jaiswal, A. K., Goda, J. S., Purwar, R. (2022) Combinatorial approaches to effective therapy in glioblastoma (GBM): current status and what the future holds. *Int. Rev. Immunol.* **41**, 582-605.

Bugno, M., Daniel, M., Chepelev, N. L., Willmore, W. G. (2015) Changing gears in Nrf1 research, from mechanisms of regulation to its role in disease and prevention. *Biochim. Biophys. Acta* **1849**, 1260-1276.

Dalavaikodihalli Nanjaiah, N., Ramaswamy, P., Goswami, K., Fathima, K. H., Borkotokey, M. (2019) Survival of glioblastoma cells in response to endogenous and exogenous oxidative challenges: possible implication of NMDA receptor-mediated regulation of redox homeostasis. *Cell Biol. Int.* **43**, 1443-1452.

Grochans, S., Cybulska, A. M., Simińska, D., Korbecki, J., Kojder, K., Chlubek, D., Baranowska-Bosiacka, I. (2022) Epidemiology of glioblastoma multiforme - literature review. *Cancers (Basel)* **14**, 2412.

Hayes, J. D., Dinkova-Kostova, A. T., Tew, K. D. (2020) Oxidative stress in cancer. *Cancer Cell* **38**, 167-197.

Herring, J. A., Elison, W. S., Tessem, J. S. (2019) Function of Nr4a orphan nuclear receptors in proliferation, apoptosis and fuel utilization across tissues. *Cells* **8**, 1373.

Hu, S., Feng, J., Wang, M., Wufuer, R., Liu, K., Zhang, Z., Zhang, Y. (2022) Nrf1 is an indispensable redox-determining factor for mitochondrial homeostasis by integrating multi-hierarchical regulatory networks. *Redox Biol.* **57**, 102470.

Jelic, M. D., Mandic, A. D., Maricic, S. M., Srdjenovic, B. U. (2021) Oxidative stress and its role in cancer. *J. Cancer Res. Ther.* **17**, 22-28.

Kuo, C. L., Ponneri Babuharisankar, A., Lin, Y. C., Lien, H. W., Lo, Y. K., Chou, H. Y., Tangeda, V., Cheng, L. C., Cheng, A. N., Lee, A. Y. (2022) Mitochondrial oxidative stress in the tumor microenvironment and cancer immunoescape: foe or friend? *J. Biomed. Sci.* **29**, 74.

Li, W., Li, X., Wang, W., Li, X., Tan, Y., Yi, M., Yang, J., McCarthy, J. B., Xiong, W., Wu, M., Ma, J., Su, B., Zhang, Z., Liao, Q., Xiang, B., Li, G. (2011) NOR1 is an HSF1- and NRF1-regulated putative tumor suppressor inactivated by promoter hypermethylation in nasopharyngeal carcinoma. *Carcinogenesis* **32**, 1305-1314.

McNamara, C., Mankad, K., Thust, S., Dixon, L., Limback-Stanic, C., D'Arco, F., Jacques, T. S., Löbel, U. (2022) 2021 WHO classification of tumours of the central nervous system: a review for the neuroradiologist. *Neuroradiology* **64**, 1919-1950.

Northrop, A., Byers, H. A., Radhakrishnan, S. K. (2020) Regulation of NRF1, a master transcription factor of proteasome genes: implications for cancer and neurodegeneration. *Mol. Biol. Cell* **31**, 2158-2163.

Olivier, C., Oliver, L., Lalier, L., Vallette, F. M. (2020) Drug resistance in glioblastoma: the two faces of oxidative stress. *Front. Mol. Biosci.* **7**, 620677.

Ostrowski, R. P., Pucko, E. B. (2022) Harnessing oxidative stress for anti-glioma therapy. *Neurochem. Int.* **154**, 105281.

Pla-Martín, D., Schatton, D., Wiederstein, J. L., Marx, M., Rugarli, E. I. (2020) CLUH granules coordinate translation of mitochondrial proteins with mTORC1 signaling and mitophagy. *EMBO J.* **39**, e102731.

Rong, L., Li, N., Zhang, Z. (2022) Emerging therapies for glioblastoma: current state and future directions. *J. Exp. Clin. Cancer Res.* **41**, 142.

Ruvkun, G., Lehrbach, N. (2023) Regulation and functions of the ER-associated Nrf1 transcription factor. *Cold Spring Harb. Perspect. Biol.* **15**, a041266.

Sun, L., Ouyang, N., Shafi, S., Zhao, R., Pan, J., Hong, L., Song, X., Sa, X., Zhou, Y. (2023) NRF1 regulates the epithelial mesenchymal transition of breast cancer by modulating ROS homeostasis. *Technol. Cancer Res. Treat.* **22**, 15330338231161141.

Sun, Q., Li, S., Wang, Y., Peng, H., Zhang, X., Zheng, Y., Li, C., Li, L., Chen, R., Chen, X. (2018) Phosphoglyceric acid mutase-1 contributes to oncogenic mTOR-mediated tumor growth and confers non-small cell lung cancer patients with poor prognosis. *Cell Death Differ*. **25**, 1160-1173.

Xu, Y., Tokar, E. J., Sun, Y., Waalkes, M. P. (2012) Arsenic-transformed malignant prostate epithelia can convert non-contiguous normal stem cells into an oncogenic phenotype. *Environ. Health Perspect.* **120**, 865-871.

Yuan, J., Zhang, S., Zhang, Y. (2018) Nrf1 is paved as a new strategic avenue to prevent and treat cancer, neurodegenerative and other diseases. *Toxicol. Appl. Pharmacol.* **360**, 273-283.

Yuan, B., Wang, G., Tang, X., Tong, A., Zhou, L. (2022) Immunotherapy of glioblastoma: recent advances and future prospects. *Hum. Vaccin. Immunother.* **18**, 2055417.

Zhang, Y., Xiang, Y. (2016) Molecular and cellular basis for the unique functioning of Nrf1, an indispensable transcription factor for maintaining cell homoeostasis and organ integrity. *Biochem. J.* **473**, 961-1000.

Zhang, S., Deng, Y., Xiang, Y., Hu, S., Qiu, L., Zhang, Y. (2020) Synergism and antagonism of two distinct, but confused, Nrf1 factors in integral regulation of the nuclear-to-mitochondrial respiratory and antioxidant transcription networks. *Oxid. Med. Cell. Longev.* **2020**, 5097109.